## NEUROSCIENCE

# Calpain-2 as a therapeutic target in repeated concussion–induced neuropathy and behavioral impairment

Yubin Wang[1], Yan Liu[1], Amy Nham[1], Arash Sherbaf[1], Diana Quach[1], Emad Yahya[1], Davis Ranburger[1], Xiaoning Bi[2], Michel Baudry[1]*

Repeated concussion represents a serious health problem as it can result in various brain pathologies, ranging from minor focal tissue injury to severe chronic traumatic encephalopathy. The calcium-dependent protease, calpain, participates in the development of neurodegeneration following concussion, but there is no information regarding the relative contribution of calpain-1 and calpain-2, the major calpain isoforms in the brain. We used a mouse model of repeated concussions, which reproduces most of the behavioral and neuropathological features of the human condition, to address this issue. Deletion of calpain-2 or treatment with a selective calpain-2 inhibitor for 2 weeks prevented most of these neuropathological features. Changes in TAR DNA binding protein 43 (TDP-43) subcellular localization similar to those found in human amyotrophic lateral sclerosis and frontotemporal dementia were also prevented by deletion of calpain-2 or treatment with calpain-2 inhibitor. Our results indicate that a selective calpain-2 inhibitor represents a therapeutic approach for concussion.

## INTRODUCTION

Traumatic brain injury (TBI) is a serious public health problem in the United States. In 2013 alone, an estimated 2.8 million TBI cases presented for treatment, and it is likely that many more cases were never reported (www.cdc.gov/traumaticbraininjury/get_the_facts. html). The cause of injury varies greatly and includes motor vehicle accidents, falls, sport injuries, and gunshot wounds, to name a few. The severity of TBI is generally classified as mild (1), also called concussion, moderate, and severe, which is often associated with a prolonged period of unconsciousness after the injury. TBI induces immediate and prolonged neuropathological consequences, including axonal damage (2) and neuronal death (3). In recent years, repeated mild TBI (rmTBI) has received a lot of attention after it was found that many athletes subjected to repeated concussions exhibit a chronic degenerative disease referred to as chronic traumatic encephalopathy (CTE) (4). CTE is characterized by massive accumulation of hyperphosphorylated tau, gliosis, and neurodegeneration (5).

Numerous reviews have discussed the role of calpain in neurodegeneration (6, 7) in general and more specifically, in stroke (8, 9) and TBI (10, 11). Consequently, numerous studies have evaluated the use of calpain inhibitors to reduce neurodegeneration in both stroke and TBI (12, 13, 14). While some studies have reported some positive effects of calpain inhibitors in TBI (15), other studies have not confirmed these results. In particular, overexpression of the endogenous calpain inhibitor, calpastatin, was reported to reduce the formation of spectrin breakdown product (SBDP) (9), resulting from calpain-mediated truncation of spectrin, a widely used biomarker of calpain activation and potentially of neurodegeneration (16), but had no effect on neurodegeneration (17). Recent studies concluded that two calpain inhibitors, SNJ-1945 and MDL-28170, which are blood-brain barrier and cell permeable, did not have sufficient efficacy or a practical therapeutic window in a widely used TBI model,

referred to as the controlled cortical impact (CCI) model (15, 18). While those non–isoform-selective calpain inhibitors were shown to inhibit overall calpain activation (without distinguishing which calpain isoform was targeted) following TBI, they failed to provide neuroprotection.

Diffuse axonal degeneration has been shown to be responsible for many of the long-term functional consequences of mTBI (1, 19). Calpain activation has been repeatedly shown to be involved in diffuse axonal injury, as calpain-mediated proteolysis of spectrin has been observed 1 to 2 hours after injury. Blood levels of the calpain-mediated N-terminal fragment of spectrin were found to be elevated shortly after injury and predicted the long-term consequences of the injury in patients with mTBI, including professional hockey players experiencing concussions (20, 21). While all the evidence strongly supports a role for calpain in mTBI, there is little information regarding which of the calpain isoforms is responsible for producing the neuropathological consequences of mTBI or rmTBI. We previously proposed that calpain-1 activation was neuroprotective, while calpain-2 activation was neurodegenerative and provided evidence for such opposite functions of these two calpain isoforms in the CCI mouse model of TBI (22). Here, we report that calpain-2 conditional knockout (C2CKO) mice are remarkably protected against the pathological consequences of rmTBI. Moreover, semichronic treatment of wild-type (WT) mice with a selective calpain-2 inhibitor results in a similar level of protection in the rmTBI mouse model. In this model, the amyotrophic lateral sclerosis (ALS) and frontotemporal lobar degeneration (FTLD) marker, TDP-43, exhibits changes in subcellular localization similar to those found in these patients, and these changes are also prevented by either genetic deletion or pharmaceutical inhibition of calpain-2. These results strongly suggest that a selective calpain-2 inhibitor could be a useful therapeutic treatment to prevent the long-term consequences of repeated concussions.

## RESULTS

### Decreased NMDA-induced neurotoxicity in calpain-2 KO mice

We generated C2CKO mice by crossing loxP–calpain-2 mice (obtained from the Riken Institute, Japan) with CamKII-Cre mice

[1]Graduate College of Biomedical Sciences, Western University of Health Sciences, Pomona, CA 91766, USA. [2]College of Osteopathic Medicine of the Pacific, Western University of Health Sciences, Pomona, CA 91766, USA.
*Corresponding author. Email: mbaudry@westernu.edu

(the Jackson laboratory) to produce mice with selective calpain-2 deletion in excitatory neurons from the forebrain. These mice exhibit widespread deletion of calpain-2 in the majority of neurons in the cortex and almost complete elimination of calpain-2 in hippocampus (Fig. 1A and fig. S1A). We previously reported that N-methyl-D-aspartate (NMDA)–mediated neurotoxicity in acute hippocampal slices prepared from juvenile mice was exacerbated in calpain-1 KO mice but reduced in the presence of a calpain-2 inhibitor (23). To further corroborate the role of calpain-2 in NMDA-mediated neurotoxicity, we tested the effects of NMDA treatment of hippocampal slices from 2-week-old WT or from C2CKO mice on neuronal injury. As previously reported, NMDA treatment resulted in a significant increase in lactate dehydrogenase (LDH) release in the incubation medium, a well-recognized marker of neurotoxicity (Fig. 1B). The effect was significantly reduced in the slices from C2CKO mice, thereby confirming the role of calpain-2 activation in NMDA-mediated neurotoxicity. NMDA receptor–mediated neurotoxicity has been extensively studied in TBI models (24). We compared the extent of brain lesion in WT and C2CKO mice in the CCI model of TBI. Lesion volume was significantly reduced in the brain of C2CKO mice as compared to WT mice (fig. S1, B and C). These results further support the role of calpain-2 activation in NMDA receptor–mediated neurotoxicity in vivo.

## Calpain-2 activation following repeated mild concussions in WT and C2CKO mice

We previously reported that calpain-2 played a significant role in the CCI model of TBI in mice (22). To analyze the potential role of calpain-2 in rmTBI, we used the repetitive concussion model developed by Petraglia and colleagues (25, 26). In this model, awake mice are subjected to four daily hits on the head for 10 consecutive days (see Materials and Methods). We first determined the time course of calpain activation in the brain in this model. Animals were sacrificed at various times after the last impact, and levels of the SBDP generated by calpain activation in cortex and hippocampus were determined (Fig. 1, C to F). In WT mice, SBDP levels in the cortex ipsilateral from the impact were elevated 24 hours and 3 days after the last impact. They were still slightly elevated 7 days after the last impact. Similar results were found in ipsilateral hippocampus. In contrast, there was no increase in SBDP levels at any time in cortex or hippocampus from C2CKO mice. We also analyzed the time course of the exposure of the phosphatase-activated domain (PAD) of tau, which appears early in tauopathy (fig. S1, D to G) (27, 28). In control animals, the changes in PAD-tau were quite similar to those found in SBDP in both cortex and hippocampus, with small variation in statistical significance. In contrast, there were no changes in phospho–PAD-tau in cortex and hippocampus from C2CKO mice after rmTBI.

## Pathological changes following repeated concussions in WT and C2CKO mice

Previous studies using the same model of repeated concussions have shown that mice exhibited a number of behavioral impairments, including cognitive impairment, as well as many pathological changes, such as activation of astrocytes and microglia in various brain regions and axonal degeneration mostly localized to the corpus callosum and the optic tract (24). At 1 and 3 months after the last concussion, WT mice exhibited depressed behavior after the last concussion, as

evidenced in the tail suspension test in which mice subjected to repeated concussions became immobile much faster than the sham mice (Fig. 2, A and B); in contrast, C2CKO mice did not exhibit any of these behavioral alterations. We also tested the loxP-calpain-2 mice (control for C2CKO) and found that they behave very similarly to the WT mice. At 1 and 3 months after repeated concussions, WT mice exhibited increased risk-taking behavior in the elevated plus maze, as evidenced by increased time spent in the open arms and increased number of entries in open arms (Fig. 2, C to F). This behavioral alteration was completely absent in C2CKO mice. Again, control mice behave similarly to WT mice. Last, we tested mice for cognitive impairment at 1 and 3 months after repeated concussions, using hippocampus-dependent fear conditioning. While WT and control mice exhibited significant impairment in learning and memory, C2CKO mice did not exhibit any significant deficits (Fig. 2, G and H). We also analyzed changes in motor function immediately and for 2 weeks after the last concussion using the beam-walking test, which has previously been used to detect the effects of concussion on speed and balance. Repeated concussions produced a relatively mild impairment, as evidenced by increase in both the time to cross the beam and the number of foot slips at 1 hour, 1 day, and 4 days after the last concussion. WT mice recovered 7 days later (fig. S2, A and B). While C2CKO mice performed a little better than WT, the differences were not statistically significant.

A major pathological hallmark of repeated concussions is brain inflammation reflected by activation of both astrocytes and microglia (1). We analyzed astrocyte and microglia activation in the brain at 3 months following repeated concussions. We used immunohistochemistry (IHC) to label glial fibrillary acidic protein (GFAP)–positive astrocytes (Fig. 3A and fig. S3) and Iba-1–positive microglia (Fig. 3C and fig. S4) and quantitatively determined the numbers of reactive astrocytes and activated microglia, as described in Materials and Methods. The numbers of reactive astrocytes and activated microglia were significantly increased in hippocampus and cortex of WT and control mice (Fig. 3, B and D, and figs. S3 and S4). In contrast, C2CKO mice did not exhibit any significant increase in number of reactive astrocytes or activated microglia.

Another hallmark of repeated concussions is axonal degeneration in various neuronal tracts (1). We used Gallyas staining to visualize axonal degeneration 3 months after repeated concussions (Fig. 3, E and F). Axonal degeneration was prominent in the optic tract in WT and control mice subjected to repeated concussions. No significant axonal degeneration was observed in C2CKO mice after repeated concussions. Image analysis was used to quantify the results and confirmed the significant axonal degeneration following repeated concussions in WT and control mice and its absence in C2CKO mice. Neuronal loss has also been observed in some models of repeated concussions (29). We therefore determined the number of neurons in various brain structures following repeated concussions in WT mice. Under our experimental conditions, we did not detect a significant decrease in the number of NeuN-positive cells in various brain regions 3 months following repeated concussions in WT mice (fig. S5, A to C).

## Changes in tau pathology and TDP-43 following repeated concussions in WT and C2CKO mice

As mentioned above, one of the hallmarks of CTE is a massive increase in tau hyperphosphorylation at various residues in various brain regions. We had previously observed tau hyperphosphorylation
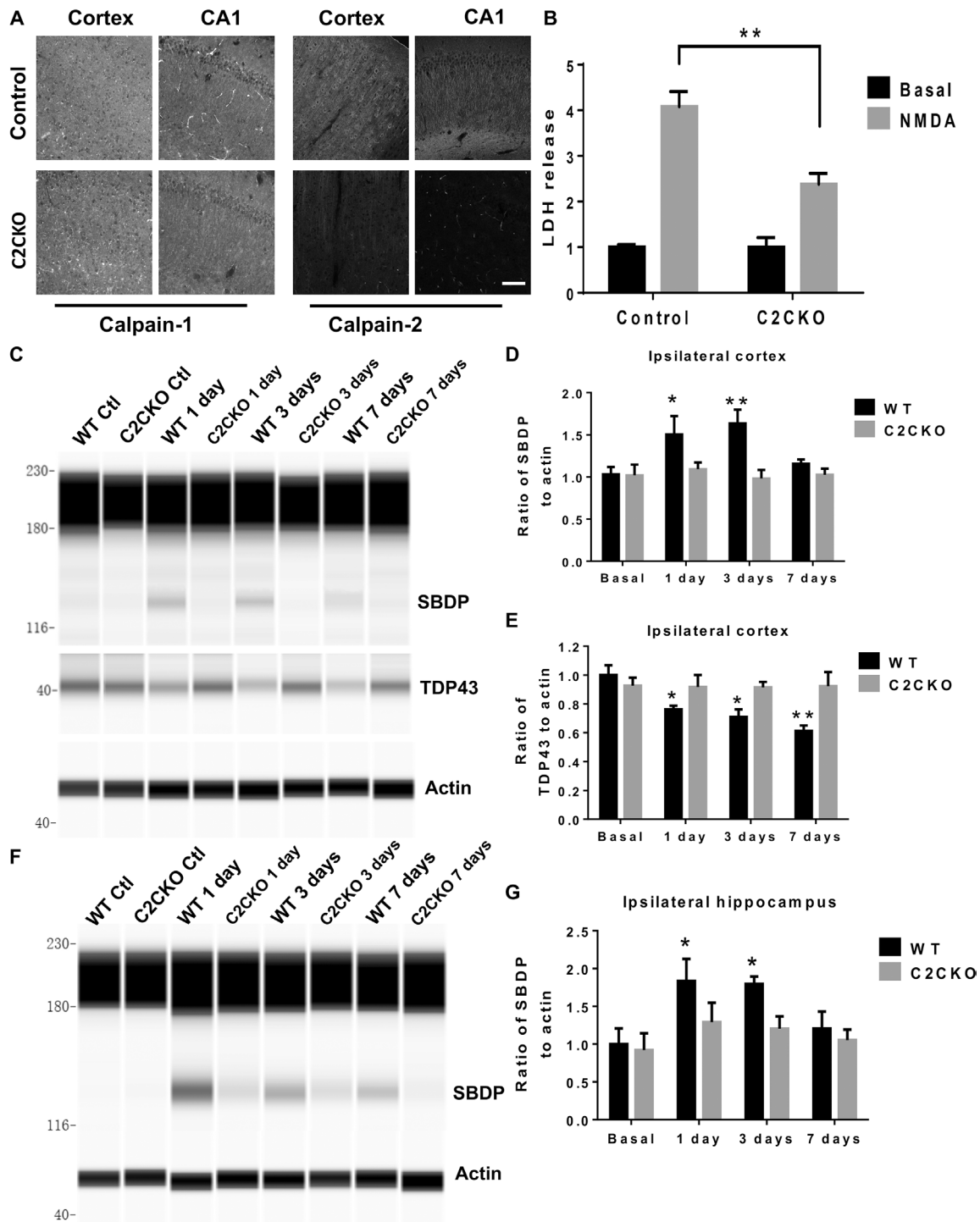
**Fig. 1. Calpain-2 deletion in C2CKO mice and time course of calpain-2 activation in cortex and hippocampus after repeated concussions.** (**A**) Calpain-2 deletion in cortex and hippocampus in C2CKO mice. loxP-Calpain-2 mice were crossed with CamKII-Cre mice to generate mice with calpain-2 deletion in excitatory neurons of the forebrain. Note the very large decrease in calpain-2 immunoreactivity in cortex and field CA1 of hippocampus and the absence of changes in calpain-1 staining. Scale bar, 50 μm. (**B**) Reduced NMDA-mediated toxicity in acute hippocampal slices from C2CKO mice. Hippocampal slices were prepared from 3-week-old WT or C2CKO mice. They were incubated with NMDA (100 μM) for 2.5 hours, and lactate dehydrogenase (LDH) release in the medium was assayed. Results represent means ± SEM of four experiments. **$P < 0.01$. Two-way analysis of variance (ANOVA) followed by Bonferroni's test. (**C** and **F**) Changes in spectrin and TDP-43 in ipsilateral cortex (C) and hippocampus (F) at various times after the last concussion in WT and C2CKO mice. WT and C2CKO mice were subjected to 10 days of repeated concussions. They were sacrificed 1, 3, and 7 days after the last day of treatment, and levels of the SBDP generated by calpain activation and full-length TDP-43 were determined by Western blot analysis. (**D**, **E**, and **G**) Quantification of the Western blot data for ipsilateral cortex [(D) and (E)] and ipsilateral hippocampus (G). Results represent means ± SEM of four experiments. *$P < 0.05$, **$P < 0.01$ compared to WT basal. Two-way ANOVA followed by Bonferroni's test. Ctl, control.
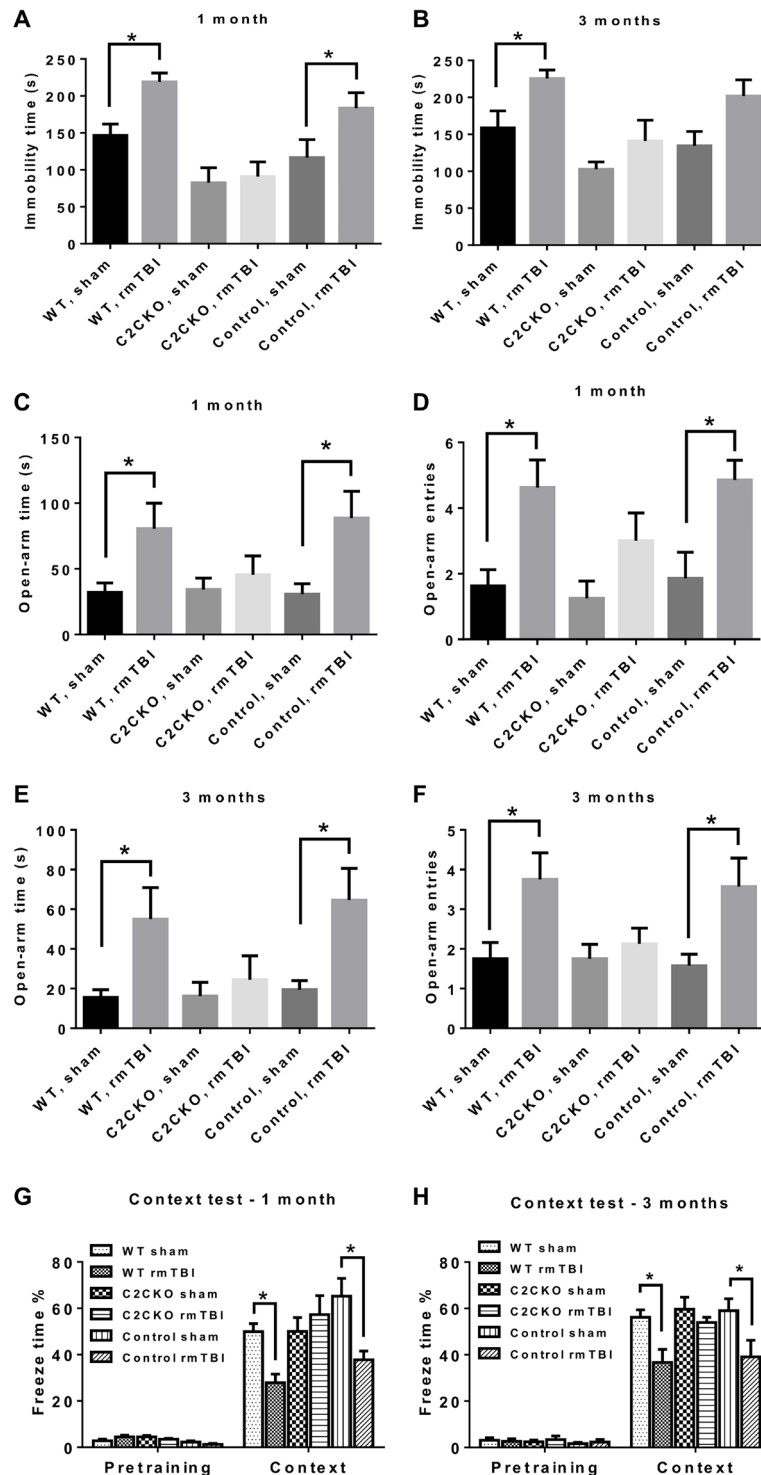
**Fig. 2. Behavioral changes in WT, C2CKO, and control mice following repeated concussions.** (**A** and **B**) Changes in tail suspension task at 1 (A) and 3 (B) months after repeated concussions. Groups of sham and rmTBI WT, C2CKO, and control mice were suspended by the tail for 5 min. The time during which the animals remained immobile was recorded. $n = 9$ for WT and C2CKO groups, and $n = 8$ for control groups. Results are means ± SEM. *$P < 0.05$. One-way ANOVA followed by Bonferroni's test. (**C** to **F**) Changes in plus-elevated maze at 1 [(C) and (D)] and 3 [(E) and (F)] months after repeated concussions. Groups of sham and rmTBI WT, C2CKO, and control mice were placed in an elevated plus maze, and the time spent in open arms [(C) and (E)] and number of entries in open arms [(D) and (F)] were recorded. $n = 9$ for WT and C2CKO groups, and $n = 8$ for control groups. Results are means ± SEM. *$P < 0.05$. One-way ANOVA followed by Bonferroni's test. (**G** and **H**) Performance in fear conditioning test at 1 (G) and 3 (H) months after repeated concussions. Groups of sham and rmTBI WT, C2CKO, and control mice were trained in the context test of the fear conditioning task. They were tested the following day, and the percent freezing time over 5-min test was recorded. $n = 8$ for WT and C2CKO groups, and $n = 7$ for control groups. Results are means ± SEM. *$P < 0.05$. One-way ANOVA followed by Bonferroni's test.
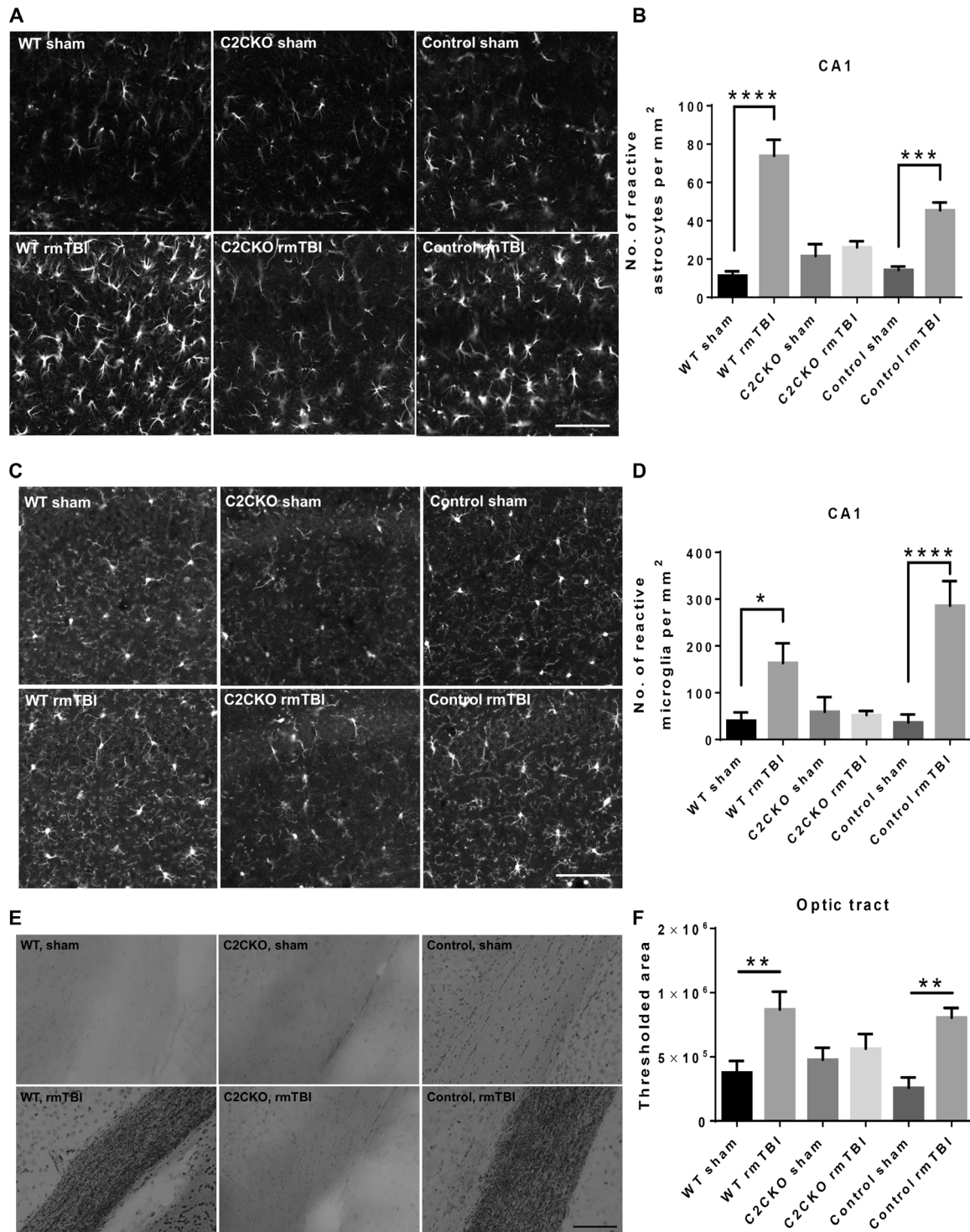
**Fig. 3. Changes in glial activation and axonal degeneration in WT, C2CKO, and control mice 3 months after repeated concussions.** Groups of sham and rmTBI WT, C2CKO, and control mice were sacrificed 3 months after repeated concussions. (**A**) Changes in astrocyte activation in field CA1 of hippocampus. Brains were fixed and processed for IHC with GFAP antibodies. Scale bar, 100 μm. (**B**) Quantification was performed, as described in Materials and Methods. $n = 8$ for WT and C2CKO groups, and $n = 7$ for control groups. ***$P < 0.001$ and ****$P < 0.0001$. One-way ANOVA followed by Bonferroni's test. Data represent means ± SEM. (**C**) Changes in microglia activation in field CA1 of hippocampus. Brains were fixed and processed for IHC with iba-1 antibodies. Scale bar, 100 μm. (**D**) Quantification was performed, as described in Materials and Methods. $n = 8$ for WT and C2CKO groups, and $n = 7$ for control groups. *$P < 0.05$ and ****$P < 0.0001$. One-way ANOVA followed by Bonferroni's test. Data represent means ± SEM. (**E**) Changes in axonal degeneration in the optic tract. Brains were fixed and processed for Gallyas staining. Scale bar, 100 μm. (**F**) Quantification was performed, as described in Materials and Methods. $n = 6$. **$P < 0.01$. One-way ANOVA followed by Bonferroni test. Data represent means ± SEM.

in the CCI mouse model of TBI and proposed the hypothesis that this effect was triggered at least, in part, by calpain-2–mediated cleavage of the tyrosine phosphatase, PTPN13, and the resulting activation of c-Abl (22). In the present study, massive increase in tau phosphorylation at threonine 231 was present in cortex, corpus callosum, and optic tract 3 months after rmTBI in WT and control mice (Fig. 4, A to F). On the other hand, no significant changes in tau phosphorylation were detected in C2CKO mice. TDP-43 is an RNA/DNA binding protein, which accumulates in neurons in ALS and FTLD (30). One of the hypotheses for its accumulation in these diseases is that TDP-43 is partially cleaved by calpain, preventing its nuclear transport and inducing its cytosol accumulation and aggregation (31). We therefore determined changes in cortical levels of TDP-43 following rmTBI in WT and C2CKO mice at 1, 3, and 7 days after repeated concussions (Fig. 1, C and E). TDP-43 levels were significantly decreased at these three time points in WT mice but were unchanged in C2CKO mice. In cortex, phospho–TDP-43 (p-TDP-43), the pathological form of TDP-43, exhibited changes in subcellular localization, with accumulation in the cytoplasm and decreased expression in the nucleus, where it is found under control conditions (Fig. 4, G and H), which were very similar to what has been reported in human patients with ALS or FTLD (30). These changes in p-TDP-43 localization were completely absent in C2CKO mice (Fig. 4, G and H).

## Effects of a selective calpain-2 inhibitor following repetitive concussions in WT mice

We previously identified a relatively selective calpain-2 inhibitor, C2I (32), which provides a significant degree of protection against pathological changes in the CCI mouse model of TBI, when injected intraperitoneally after TBI (22). For the present study, in which repeated concussions were administered over a period of 10 days, we selected to deliver C2I through subcutaneously implanted Alzet minipumps. We first verified that this mode of delivery was effective to inhibit calpain-2–mediated neurodegeneration in cortex in the CCI model (fig. S5, D and E). The pumps were then implanted the day before the start of the concussions and were withdrawn after 2 weeks. Animals were tested for motor impairment immediately at the end of the repeated concussions and for cognitive impairment 1 month later. They were then sacrificed, and the same pathological markers used previously were analyzed. Animals treated with C2I were significantly protected against the depression symptom (fig. S6A), the risk-taking behavior (fig. S6, B and C), and cognitive impairment, assessed with novel object location (fig. S6D) and hippocampus-dependent fear conditioning (fig. S6E). These results were quite similar to those observed in the C2CKO mice, although the animals were tested 1 month after the last concussion. We also analyzed changes in motor function immediately and for 2 weeks following the last concussion using the beam-walking test (fig. S2, C and D). The results in animals treated with C2I were very similar to those we observed in C2CKO mice; and although C2I-treated animals performed slightly better than vehicle-treated animals, the differences were not statistically significant. Astrogliosis, microglial activation, and axonal degeneration were analyzed 1 month after the last concussion (Fig. 5). Animals treated with C2I did not exhibit significant astroglial (Fig. 5, A and B) and microglial (Fig. 5, C and D) activation in field CA1; they also did not show astroglial or microglial activation in CA3, dentate gyrus, or cortex (figs. S7 and S8). Axonal degeneration 1 month after concussion was observed in the optic tract (Fig. 5, E and F) in vehicle-treated animals but was not significantly changed in animals treated with C2I. We also observed axonal degeneration in cortex and in corpus callosum 1 month after the last concussion in vehicle-treated animals, and this effect was much reduced by C2I treatment (fig. S9). One month after the last concussion increased tau phosphorylation was observed in various brain regions in vehicle-treated animals, including cortex (Fig. 6, A and B), corpus callosum (Fig. 6, C and D), and optic tract (Fig. 6, E and F). These changes in tau phosphorylation were absent in animals treated with C2I. Changes in p-TDP-43 subcellular localization were also observed 1 month after the last concussion in cortex, with p-TDP-43 being almost exclusively translocated from the nucleus to the cytoplasm (fig. S10, A and B). TDP-43 subcellular localization was not significantly altered in C2I-treated mice. Last, levels of p-TDP-43 were significantly increased after rmTBI in the optic tract (fig. S10, C and D), suggesting abnormal processing of p-TDP-43 in the axons of retinal ganglion cells. Levels of p-TDP-43 in the optic tract were not significantly increased after rmTBI in C2I-treated mice.

## DISCUSSION

Our results demonstrate that calpain-2 activation plays a critical role in the development of neuropathology following repeated concussions. Thus, both the functional impairment and the pathological manifestations of brain damage, including inflammation, axonal degeneration, and tau and TDP-43 abnormalities, were absent in mice with genetic calpain-2 deletion or treatment with a relatively selective calpain-2 inhibitor. One of the difficulties to identify novel therapeutic treatments for neurological diseases has been the lack of reproducibility in the animal models used in various laboratories. It is therefore reassuring that our results in the mouse model of repeated mild concussions are in excellent agreement with the findings reported by Petraglia et al. (25, 26) and others (1). Thus, we observed early impairment in motor function, which rapidly recovered, and changes in depression symptoms and risk-taking behavior similar to those previously reported. While previous studies have used the Morris water maze to analyze changes in cognitive behavior, we used fear conditioning as an index of cognition and also observed changes in performance in this paradigm, confirming that rmTBI results in impaired cognition. We observed widespread astroglia and microglia activation at 1 and 3 months after the last concussion. We identified reactive astrocytes on the basis of their larger size and number of processes (33) and quantified their numbers in various brain regions. Our results demonstrated increased numbers of reactive astrocytes at 1 and 3 months after repeated concussions. In contrast, there was no increase in the numbers of reactive astrocytes in C2CKO mice or after treatment with the selective calpain-2 inhibitor. Similarly, we identified reactive microglia on the basis of larger and irregular soma (34) and quantified their numbers in various brain regions after repeated concussions. Our results indicated that there was a significant increase in the numbers of reactive microglia after repeated concussions in WT and control mice but no increase following down-regulation of calpain-2 or pharmacological inhibition. Increased tau phosphorylation was present in various brain regions, as previously reported in various models of mTBI (35). Axonal degeneration was present in corpus callosum and optic tract, in good agreement with previous reports (26). While some neuronal degeneration has been reported in some model of repeated concussions (29), we did not observe any significant neuronal loss
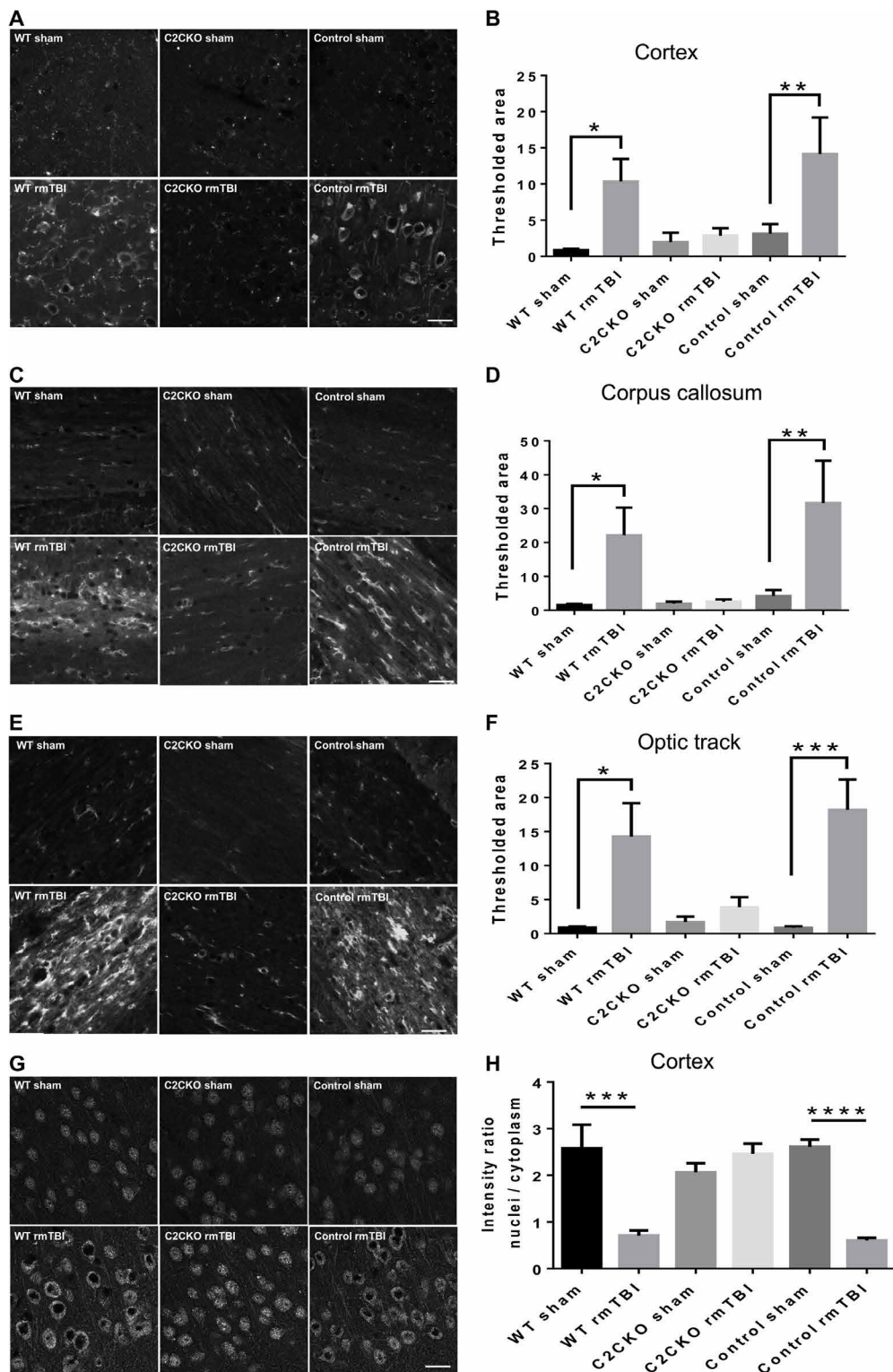
**Fig. 4. Changes in tau phosphorylation and in TDP-43 localization in WT, C2CKO, and control mice 3 months after repeated concussions.** Groups of sham and rmTBI WT, C2CKO, and control mice were sacrificed 3 months after repeated concussions. (**A**, **C**, and **E**) Changes in tau phosphorylation in cortex, corpus callosum, and optic tract. Brains were fixed and processed for IHC with phospho-tau (p-tau) Thr[231] antibodies. Scale bars, 20 μm. (**B**, **D**, and **F**) Quantification of images similar to those shown. $n = 6$ for WT sham; $n = 7$ for C2CKO sham, control sham, and control rmTBI; $n = 8$ for WT rmTBI and C2CKO rmTBI. *$P < 0.05$, **$P < 0.01$, and ***$P < 0.001$. One-way ANOVA followed by Bonferroni's test. Data represent means ± SEM. (**G**) Changes in phospho–TDP-43 (p-TDP-43) subcellular localization in cortex. Brains were fixed and processed for IHC with a p-TDP-43 Ser[409]/Ser[410] antibody. Scale bar, 20 μm. (**H**) Quantification of the p-TDP-43 intensity ratio of nuclei to cytoplasm. $n = 4$. ***$P < 0.001$ and ****$P < 0.0001$. One-way ANOVA followed by Bonferroni's test. Data represent means ± SEM.
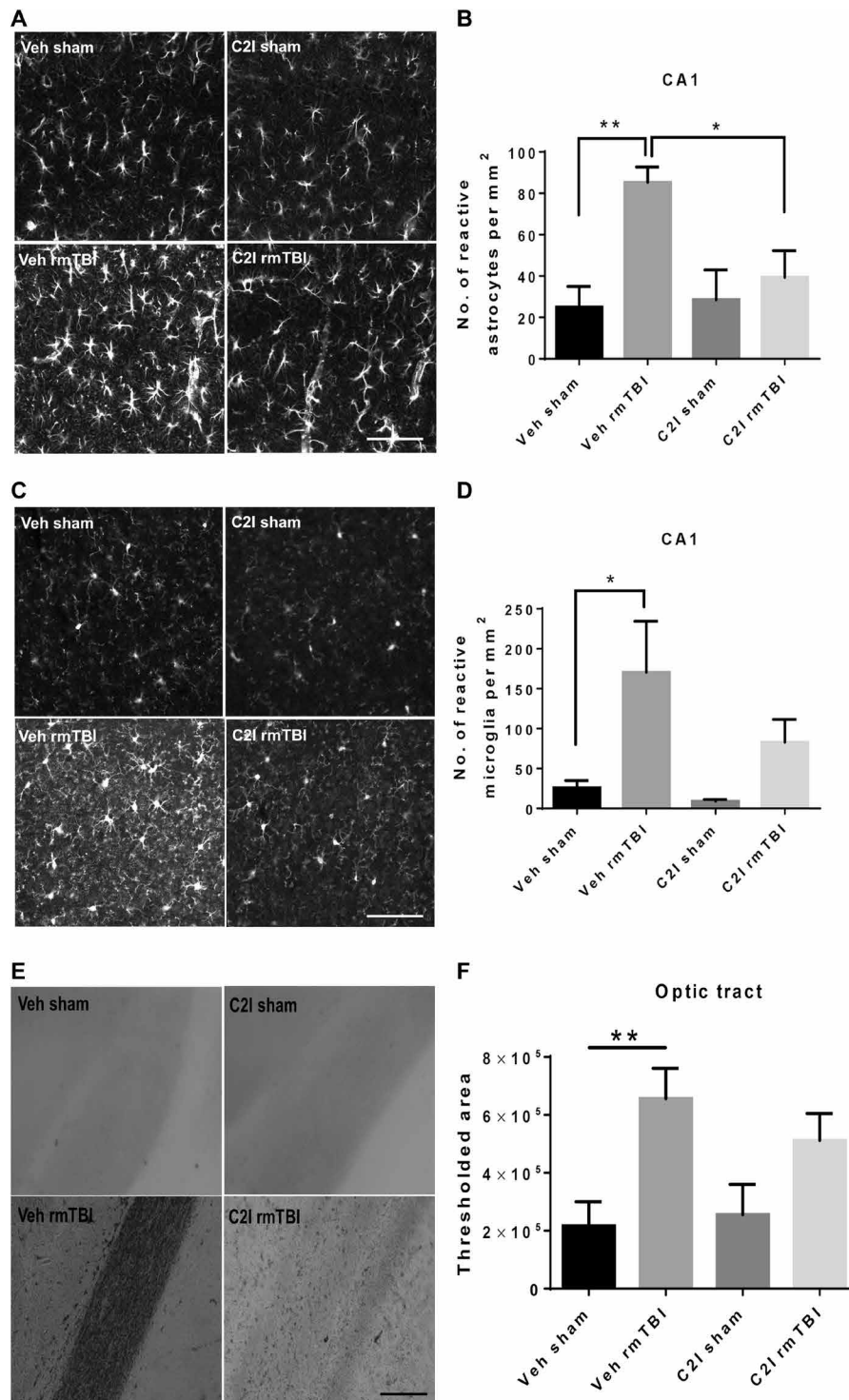
**Fig. 5. Effects of C2I treatment on glial activation and axonal degeneration following repeated concussions in WT mice.** WT mice were implanted with Alzet minipumps delivering vehicle [veh; 400 mg/ml; (2-hydroxypropyl)-β-cyclodextrin] or C2I (0.3 mg kg$^{-1}$ day$^{-1}$) 1 day before 10 days of repeated concussions. Pumps were withdrawn 4 days after the last day of concussion, and the animals were sacrificed 4 weeks later. (**A**) Changes in astrocyte activation in field CA1 of hippocampus. Brains were fixed and processed for IHC with GFAP antibodies. Scale bar, 100 μm. (**B**) Quantification of images similar to those shown. $n = 8$ for veh sham and veh rmTBI, $n = 7$ for C2I sham, $n = 9$ for C2I rmTBI. **$P < 0.01$. One-way ANOVA followed by Bonferroni's test. Data represent means ± SEM. (**C**) Changes in microglia activation in field CA1 of hippocampus. Brains were fixed and processed for IHC with iba-1 antibodies. Scale bar, 100 μm. (**D**) Quantification of images similar to those shown. $n = 8$ for veh sham and veh rmTBI; $n = 7$ for C2I sham; and $n = 9$ for C2I rmTBI. *$P < 0.05$. One-way ANOVA followed by Bonferroni's test. Data represent means ± SEM. (**E**) Changes in axonal degeneration in the optic tract. Brains were fixed and processed for Gallyas staining. Scale bar, 100 μm. (**F**) Quantification of images similar to those shown. $n = 6$. **$P < 0.01$. One-way ANOVA followed by Bonferroni's test. Data represent means ± SEM.
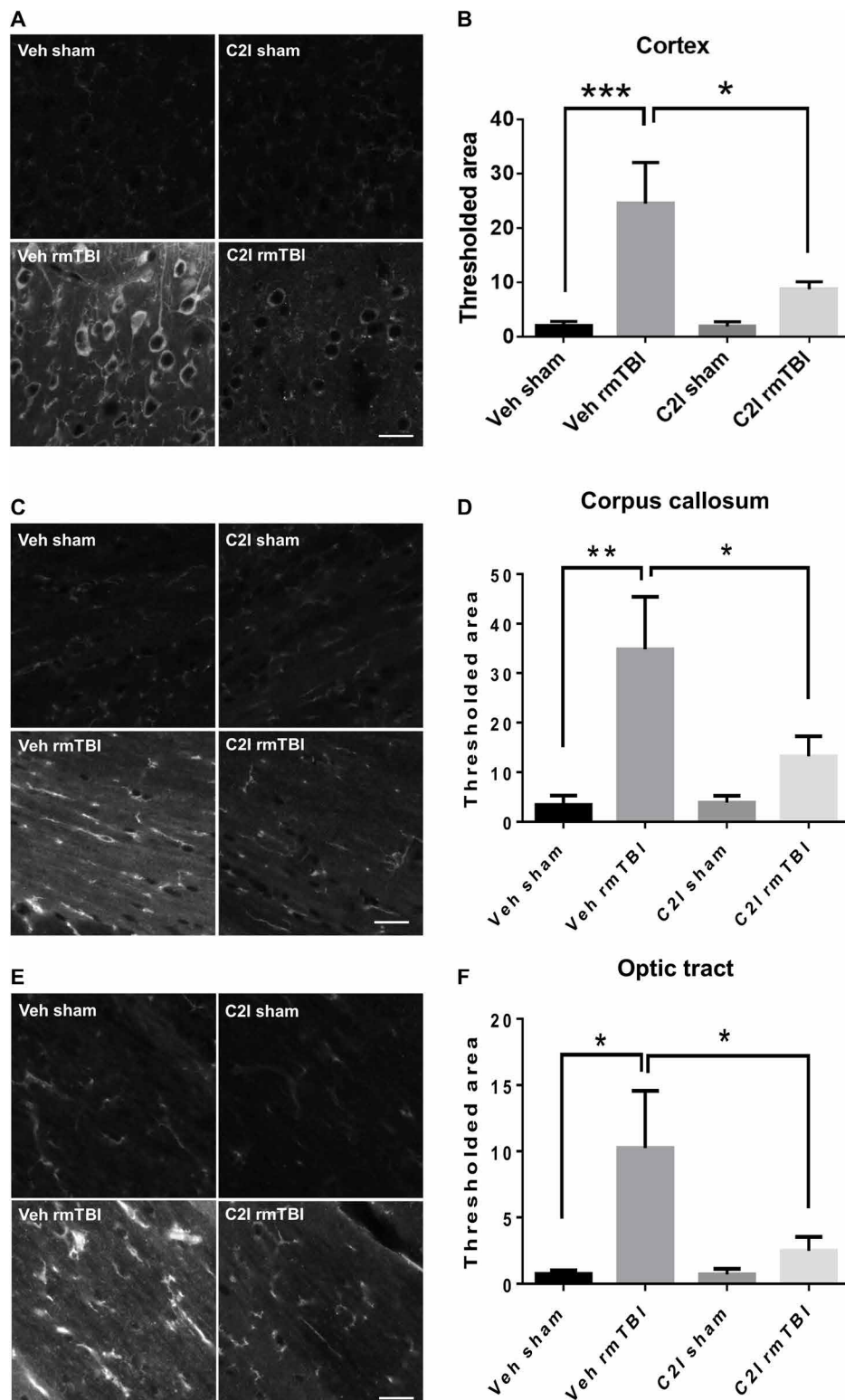
**Fig. 6. Effects of C2I treatment on changes in tau phosphorylation in WT mice 1 month after repeated concussions.** WT mice were implanted with Alzet minipumps delivering vehicle [400 mg/ml; (2-hydroxypropyl)-β-cyclodextrin] or C2I (0.3 mg kg$^{-1}$ day$^{-1}$) 1 day before 10 days of repeated concussions. Pumps were withdrawn 4 days after the last day of concussion, and the animals were sacrificed 4 weeks later. (**A**, **C**, and **E**) Changes in tau phosphorylation in cortex, corpus callosum, and optic tract. Brains were fixed and processed for IHC with p-tau Thr$^{231}$ antibodies. Scale bars, 20 μm. (**B**, **D**, and **F**) Quantification of images similar to those shown. $n = 8$ for veh sham and veh rmTBI; $n = 7$ for C2I sham; and $n = 9$ for C2I rmTBI. *$P < 0.05$, **$P < 0.01$, and ***$P < 0.001$. One-way ANOVA followed by Bonferroni's test. Data represent means ± SEM.

3 months after repeated concussions in WT mice. It is conceivable that Wallerian degeneration could take place and that neuronal loss could develop more slowly in the model we used. We also confirmed that, in this model, alterations in TDP-43, which had been previously reported in ALS and frontotemporal dementia (30), were also present in cortex. Thus, TDP-43 levels in cortex were decreased up to 7 days after repeated concussions in WT but not in C2CKO. In addition, TDP-43 exhibited changes in subcellular localization from the nucleus in control animals to the cytoplasm 3 months after repeated concussions. This change in subcellular localization has been previously discussed in relationship to calpain-mediated cleavage, leading to aggregation in the cytoplasm and contributing to the neurodegeneration observed in these disorders (35). Our findings strongly suggest that following rmTBI, TDP-43 could also be cleaved by calpain-2 and localized to the cytoplasm where aggregated TDP-43 could contribute to neurodegenerative changes. Several studies have shown that TBI can lead to CTE and ALS (3), although the potential mechanisms underlying the development of either CTE or ALS following TBI or repeated concussions are not well understood (36).

Although calpain has been repeatedly proposed to play a significant role in TBI (10, 11), there are only few data regarding the respective roles of calpain-1 and calpain-2, two of the major calpain isoforms, in TBI or concussion. We previously reported that, while calpain-1 was rapidly and transiently activated in a mouse model of TBI, calpain-2 activation was delayed and prolonged (22). Comparing the changes in SBDP in cortex and hippocampus between WT and C2CKO mice, our results indicate that in the rmTBI model, calpain-2 is activated 24 hours after the last concussion and remains activated for up to 1 week in both cortex and hippocampus. This time course of calpain-2 activation is quite similar to what we observed in the more severe TBI model we previously used. In the TBI model, we also observed that levels of calpain-2 activation were closely related to the extent of degenerating cells. In the less severe model of repeated concussions, there was no clear evidence of degenerating cells, as previously reported, suggesting that the extent of calpain-2 activation might not be sufficient to trigger cell death.

While the extent of calpain-2 activation might not have been sufficient to trigger significant cell death, it was sufficient to trigger a whole host of neurodegenerative events, including activation of astrocytes and microglia and axonal degeneration in several tracts, such as in the corpus callosum and the optic tract, since all these events were lacking in calpain-2 KO mice. These results are somewhat different from what we observed in the TBI model. In this model, we did observe massive astroglial activation 7 days after TBI in the cortex surrounding the lesion, and this was not blocked by a daily injection with a selective calpain-2 inhibitor (22). In the present study, continuous administration of the same calpain-2 inhibitor prevented glial reaction and axonal degeneration observed at 1 month after the last concussion. Reasons for this difference are currently not clear. It could be that genetic calpain-2 deletion or continuous administration of the calpain-2 inhibitor provides better calpain-2 inhibition than the daily intraperitoneal injections. It could also be related to the differences in time points selected in the two studies, since we analyzed glial activation at 1 month after concussion and not 1 week. In any event, glial activation is generally considered to have a dual effect in neurodegeneration, depending on the types of glial cells activated (37). In our studies, we did not attempt to distinguish between different subtypes of astrocytes or microglia, but it is quite remarkable that calpain-2 deletion completely eliminated both as-

trocyte and microglia activation. As previously mentioned, TBI and rmTBI have been shown to be associated with increased tau phosphorylation at various sites. We previously reported an increased tau phosphorylation at residue $Tyr^{245}$ in the CCI model of TBI, and this effect was significantly reduced following treatment with C2I (38). In the present study, we also found that calpain-2 deletion in excitatory neurons from the forebrain completely prevented rmTBI-induced increased in tau phosphorylation. We previously proposed that calpain-2–mediated truncation of the tyrosine phosphatase, PTPN13, represents a link between calpain-2 and tau phosphorylation, as one of the targets of PTPN13 is c-Abl, which can phosphorylate tau at $Tyr^{245}$. However, there are other pathways that could be regulated by calpain, including glycogen synthase kinase ß (39), which can also result in tau phosphorylation at various residues.

We used a relatively selective calpain-2 inhibitor, Z-Leu-Abu-CONH-$CH_2$-$C6H_3$ (C2I), to further confirm the role of calpain-2 in rmTBI-mediated behavioral impairments and neuropathology. Because of the duration of the repeated concussions and the prolonged activation of calpain-2 in this model, we selected to continuously deliver C2I through subcutaneously implanted minipumps, which significantly prevented calpain-2 activation in the brain following trauma. Treatment of WT mice with C2I reproduced all the beneficial effects of calpain-2 deletion at the behavioral and neuropathological levels. Thus, C2I-treated mice did not exhibit the depression symptom or the risk-taking behavior of the vehicle-treated mice. They also did not exhibit the cognitive impairment in the fear conditioning task. Activation of astrocytes and microglia was also almost completely prevented in the different brain regions tested. Likewise, increased tau phosphorylation and changes in subcellular localization of TDP-43 were almost completely blocked by C2I treatment.

## CONCLUSIONS

Our results establish that calpain-2 activation is a critical step, leading to a wide range of neuropathological changes and behavioral alterations following repeated concussions. They also demonstrate that treatment with a selective calpain-2 inhibitor represents a novel potential therapeutic approach to prevent brain damage and behavioral modifications following repeated concussions. In the present experiments, we started treatment with the selective calpain-2 inhibitor the day before the first concussion episode, and our results suggest the possibility of using a similar approach for individuals at risk for CTE, such as athletes in sport contact and military personnel. Future experiments will be directed at determining the effects of posttreatment with the inhibitor to further establish the possibility of using this treatment in human participants exposed to concussion. Considering that a blood biomarker based on calpain activation has been proposed to be a predictive diagnostic tool for human concussion, and that tau PET has recently been shown to be a useful tool to investigate neurodegeneration after TBI in human participants (40), our results further warrant pursuing the development of a selective calpain-2 inhibitor for the treatment of concussions.

## MATERIALS AND METHODS
### Study design
The objective of this study is to examine the role of calpain-2 in the pathology of repetitive mTBI. For this, we performed rmTBI or sham procedure on three groups of mice. The first group consisted

of 16 WT mice and 16 C2CKO mice. Mice were euthanized at 1, 3, and 7 days after rmTBI (four mice for each time point) or 1 day after sham procedure. Brain tissue was collected to analyze markers for calpain activation, SBDP, and for early pathological tau, PAD-tau. The second group of mice consisted of WT mice, C2CKO mice, and calpain-2 loxP mice (control for calpain-2 CKO). There were ~18 mice for each genotype (half for rmTBI and half for sham). Beam-walking tests were performed from 0 to 14 days after rmTBI. Elevated plus maze, tail suspension, and fear conditioning tests were performed at 1 and 3 months after rmTBI. The third group of mice consisted of WT mice treated with C2I or vehicle. There were ~18 mice for C2I and ~18 mice for vehicle. Beam-walking tests were performed from 0 to 14 days after rmTBI. Elevated plus maze, tail suspension, novel object, and fear conditioning tests were sequentially performed at 1 month after rmTBI. For the second and third group, mice were euthanized after behavioral tests and IHC was performed on brain sections to examine several pathological markers such as GFAP, iba-1, phospho-tau (p-tau), and p-TDP-43. Silver staining was also performed to examine neurodegeneration. In rare cases, mice showing abnormalities such as signs of pain, motor impairment, and seizures during rmTBI procedure were immediately removed from the study. Specifically, one mouse was removed from the WT rmTBI group, two mice were removed from the control rmTBI group, one mouse was removed from the vehicle rmTBI group, while no mouse was removed from the C2CKO rmTBI or C2I rmTBI group. For all behavioral and IHC studies, experiments and data analysis were done by two persons in a blind fashion.

Animal experiments were conducted in accordance with the principles and procedures of the National Institutes of Health *Guide for the Care and Use of Laboratory Animals*. All protocols were approved by the local Institutional Animal Care and Use Committee.

### Mice
We used C57Bl/6 (WT), CamKII-Cre$^{+/-}$ CAPN2$^{loxP/loxP}$ (calpain-2 CKO), and CAPN2$^{loxP/loxP}$ (loxP–calpain-2) mice, referred to as control. All mice are on a C57Bl/6 background.

### Antibodies
Primary antibodies for Western blot: SBDP (1:20; MAB1622, EMD Millipore) and PAD-tau (1:20; MABN417, EMD Millipore). Primary antibodies for IHC: calpain-1 (1:200; LS-B4768, LSBio), calpain-2 (1:300; LS-C337641, LSBio), GFAP (1:1000; AB5804, Abcam), iba-1 (1:400; AB5076, Abcam), p-tau Thr$^{231}$ (1:200; MN1040, Thermo Fisher Scientific), p-TDP-43 409/410 (1:400; 22309-1-AP, Protein-tech), and NeuN (1:200; ab104224, Abcam). Secondary antibodies for IHC: Alexa Fluor 594 goat anti-rabbit immunoglobulin G (IgG) (1:400; A11037, Thermo Fisher Scientific), Alexa Fluor 594 goat anti-mouse IgG (1:400; A11005, Thermo Fisher Scientific), and Alexa Fluor 594 donkey anti-goat IgG (1:400; A11058, Thermo Fisher Scientific).

### NMDA toxicity in acute hippocampal slices
NMDA toxicity in acute hippocampal slices from postnatal days 14 to 16 WT or C2CKO mice was analyzed, as previously described (*23*). Mice at postnatal days 14 to 16 were anesthetized with halothane and decapitated. Brains were quickly removed and transferred to oxygenated, ice-cold cutting medium: 124 mM NaCl, 26 mM NaHCO$_3$, 10 mM glucose, 3 mM KCl, 1.25 mM KH$_2$PO$_4$, 5 mM MgSO$_4$, and 3.4 mM CaCl$_2$. Hippocampal transversal slices

(400 µm thick) were prepared using a McIlwain-type tissue chopper and transferred to a recovery chamber with a modified artificial cerebrospinal fluid medium, containing: 124 mM NaCl, 2.5 mM KCl, 2.5 mM CaCl$_2$, 1.5 mM MgSO$_4$, 1.25 mM NaH$_2$PO$_4$, 24 mM NaHCO$_3$, 10 mM D-glucose, and saturated with 95% O$_2$/5% CO$_2$ for 1 hour at 37°C. Slices were then treated with NMDA (100 µM) for 3 hours. At the end of treatment, 50 µl of medium solution was transferred to a 96-well plate, and the LDH reaction was performed using the Pierce LDH Cytotoxicity Assay Kit (Thermo Fisher Scientific) following the manufacturer's instruction. To determine LDH activity, the absorbance at 680 nm (background signal) was subtracted from the absorbance at 490 nm. LDH activity was normalized to protein concentration, and results are shown as fold of controls.

### Repetitive mTBI
The rmTBI model was established in mice following the protocol described in a previous publication (*25*), with minor changes. Briefly, mice were restrained in a plastic restraint cone (89066-338, VWR International) without anesthesia and placed on a foam bed. The mouse head was not immobilized. This setting better mimics the human concussive injury, which often happens under awake conditions and the head undergoes acceleration and deceleration. A stainless steel helmet (6 mm diameter) (Millenium Machinery, Rochester, NY) was placed on the right hemisphere between the lambda and bregma. A 1.0-mm-thick double-sided gel tape (Scotch) was stick to the underside of the helmet. A pneumatically controlled impactor device (AMS-201, Amscien) was modified to deliver mild closed-head impacts. The impactor tip was replaced with a rubber round tip (6 mm diameter) to reduce the incidence of skull fracture. The impact depth was 5 mm. The impact speed was 3.5 m/s. The duration of impact was 100 ms. The impact angle was 20° from the vertical plane. After impact, mice were removed from the restraint bag and returned to their cage. Mice showing abnormalities, such as signs of pain, motor impairment, or seizures, were rarely seen and were removed from the study. Animals received four head impacts per day with a 2-hour interval between impacts for 10 days. Sham groups underwent the same procedure as the rmTBI groups. They were placed into the restraint cone on the same foam bed. However, no impacts were given.

### Osmotic pumps
Osmotic pumps (Model 2002, ALZET; release rate, 0.5 µl/hour) were filled with 200 µl of C2I (0.625 µg/µl) in (2-hydroxypropyl)-β-cyclodextrin (400 mg/ml) or with 200 µl of (2-hydroxypropyl)-β-cyclodextrin (400 mg/ml) as vehicle. Pumps were implanted subcutaneously in mice 1 day before rmTBI and removed 4 days after the last episode of rmTBI (total of 15 days). Approximately, 0.3 mg/kg of C2I was released per day. This dose is the same as the daily dose used for intraperitoneal injections of C2I in a mouse model of TBI (*22*).

### Western blot
At indicated time points after rmTBI, ipsilateral cortical and hippocampal tissues were collected from WT and C2CKO mice. Tissues were homogenized in lysis buffer (87787, Thermo Fisher Scientific), containing protease and phosphatase inhibitor cocktails (78446, Thermo Fisher Scientific), and protein concentration was measured with the bicinchoninic acid (BCA) assay (23225, Thermo Fisher

Scientific). Western blot was done using the Wes system (Protein-Simple): 1.2 μg of total protein of samples was loaded to each lane and 12 to 230 kDa separation modules were used. For the detection of PAD-tau, samples were run under nonreducing conditions. Peak areas of the bands were measured by Compass software (ProteinSimple).

## Immunohistochemistry

At 1 or 3 months after rmTBI, mice were anesthetized and intra-cardially perfused with 0.1 M phosphate buffer (pH 7.4) and then with freshly prepared 4% paraformaldehyde in 0.1 M phosphate buffer. Brains were removed and immersed in 4% paraformal-dehyde at 4°C for 1 day for postfixation and then in 15 and 30% sucrose at 4°C for 1 day each for cryoprotection. Coronal frozen sections (20 μm thick) at bregma −1.58 to −2.30 in each brain were collected. Two sections (at 160-μm interval) per animal were eval-uated for each specific immunohistochemical analysis. Sections were first blocked in 0.1 M phosphate-buffered saline (PBS) con-taining 5% goat or donkey serum and 0.3% Triton X-100 (blocking solution) for 1 hour and then incubated with primary antibody prepared in blocking solution overnight at 4°C. Sections were washed three times in PBS and incubated in Alexa Fluor secondary antibody prepared in blocking solution (1:400) for 2 hours at room temperature. After three washes, sections were mounted with mounting medium containing 4′,6-diamidino-2-phenylindole (Vector Laboratories). Sections were visualized under confocal mi-croscopy (ZEISS LSM 880). Imaging parameters were constant within each specific antigen analysis. For the quantification of reactive astrocytes, 332 μm by 332 μm areas from indicated brain regions were analyzed in each GFAP-labeled section. Image threshold was adjusted to highlight astrocytes processes. Astro-cytes with ≥4 processes visible 30 μm from the soma were consid-ered as reactive astrocytes and were manually counted in each image. For the quantification of reactive microglia, 332 μm by 332 μm areas from indicated brain regions of each iba-1–labeled section were analyzed. Image threshold was adjusted to highlight microglia soma. Microglia with soma size ≥28 μm$^2$ and circularity ≤0.6 were considered as reactive microglia and were counted using the Analyze Particles function of ImageJ. For the quantifica-tion of p-tau signals, 135 μm by 135 μm areas from indicated brain regions of each section were analyzed. The thresholded area of each image was measured using ImageJ. For the quantification of p-TDP-43 translocation, 135 μm by 135 μm areas from indicated brain regions of each section were analyzed. The ratio of the inten-sity in nuclei to the intensity in cytoplasm was calculated using an ImageJ macro named Intensity Ratio Nuclei Cytoplasm Tool. For the quantification of NeuN-positive cells, 664 μm by 249 μm areas in the lateral geniculate nucleus and parietal cortex and 166 μm by 58 μm areas in hippocampal CA1, CA3, and dentate gyrus (DG) were analyzed. Image threshold was adjusted, and NeuN-positive nuclei were counted using the Analyze Particles function of ImageJ. Image acquisition and quantification were done by two persons in a blind fashion.

## Gallyas silver staining

Coronal frozen sections (40 μm thick) at bregma −2.30 in each brain were collected. Gallyas silver staining was performed using the FD NeuroSilver Kit II (FD NeuroTechnologies). Areas (444 μm by 321 μm) at indicated brain regions of each section were imaged under a light microscope (Zeiss Axiophot). The thresholded area

of each image was measured using ImageJ. Image acquisition and quantification were done by two persons in a blind fashion.

## TUNEL staining

TUNEL (terminal deoxynucleotidyl transferase–mediated deoxyu-ridine triphosphate nick end labeling) staining was performed in a set of coronal frozen sections (20 μm thick) at bregma 0.50, −0.58, and −1.58 mm using the ApopTag in situ apoptosis detection kit (S7165, Millipore). Sections were visualized under confocal micros-copy (LSM 880, Zeiss). All TUNEL-positive nuclei surrounding the lesion area in the sections were counted using the "analyze particles" function in ImageJ. Total number of TUNEL-positive nuclei in a set of sections of each brain was summed. Image acquisition and quan-tification were done by two persons in a blind fashion.

## Beam walking

The beam apparatus consists of a 1-m wooden round beam with a diameter of 2 cm, resting 50 cm above the tabletop on two poles. A black box is placed at the end of the beam as the finish point. Nest-ing material from home cages is placed in the black box to attract the mouse to the finish point. A lamp (with 60-W light bulb) is used to shine light above the start point and serves as an aversive stimulus. Each mouse is placed on a brightly lit platform and is allowed to trans-verse the round beam. A nylon hammock is stretched below the beam, about 7.5 cm above the tabletop, to cushion any falls. On training day, mice are allowed to cross the beam, with gentle guiding or prod-ding as needed, until they cross readily. The timer is started by the nose of the mouse entering the start point and stopped when the ani-mal reaches the safe box. Mice rest for 10 min in their home cages between training sessions. Mice are trained three times. The beams and box are cleaned of mouse droppings and wiped with towels soaked with 70% ethanol and then water before the next mouse is placed on the apparatus. On testing day, mice are placed on the beam, and numbers of back paw slips and latency to cross are scored. Mice are tested three times with 10-min interval for resting. Results for the three tests are averaged to provide individual values for each mouse on that day. The experiments were performed and results analyzed by a blind observer.

## Elevated plus maze

Elevated plus maze for mice was performed following the protocol described in a previous publication (41). Briefly, the maze is painted black and consists of two open arms without walls and two closed arms with 15-cm-high walls. Each arm is 30 cm long and 5 cm wide. The maze is elevated 40 cm off of the floor. Mice were transferred to the behavioral testing room in their home cage 1 hour before the test. At the beginning of the test, mouse was placed at the center of the plus maze, facing an open arm opposite to the location of the operator. The movement of the mouse was recorded by a camera at the top of the maze for 5 min. The mouse was then returned to its home cage. The maze was cleaned with disinfectant and dried with paper towels before testing the next mouse. Video was later analyzed manually. Open-arm time, closed-arm time, open-arm entries, and closed-arm entries were counted. An arm entry was counted when all four paws of the mouse were in that arm. Behavioral test and video analysis were done by two persons in a blind fashion.

## Tail suspension

The tail suspension test was performed following the protocol de-scribed in a previous publication (42). Briefly, the tail suspension

box was made of wood and painted white. It is 55 cm high, 60 cm wide, and 11.5 cm deep. It has four compartments to test four mice at a time. A suspension bar (1 cm high, 1 cm wide, and 60 cm long) was positioned on the top of the box. Mice were transferred to the behavioral testing room in their home cage 1 hour before the test. A 17-cm-long tape was attached to the end of the mouse tail. The mice were suspended in each compartment by placing the free end of the tape on the suspension bar. The movement of the mice was recorded for 6 min by a camera in front of the tail suspension box. The mice were then returned to their home cage, and the tape was gently removed from the tail. The box was wiped with disinfectant before the next round of test. Video was later analyzed by another observer. The time that each mouse spends as mobile was measured, following the criteria described in (39). The immobility time was then calculated as total time minus mobility time. Behavioral test and video analysis were done by two persons in a blind fashion.

### Fear conditioning

For fear conditioning, we used the same protocol we used in our previous studies (22). On training day, mice were placed in the fear conditioning chamber (H10–11M-TC, Coulbourn Instruments) located in the center of a sound-attenuating cubicle (Coulbourn Instruments). After a 2-min exploration period, one tone–foot shock pairings separated by 1-min intervals were delivered. The 85-dB, 2-kHz tone lasted for 30 s, and the foot shock was 0.75 mA and lasted for 2 s. Foot shock coterminated with the tone. Mice remained in the training chamber for another 30 s before being returned to their home cages. Context test was performed 1 day after training. On day 3, animals were subjected to a cue/tone test. The same conditioning chamber was modified by changing its metal grid floor to a plastic sheet, white metal walls to plastic walls gridded with red tapes, and odor from ethanol to acetic acid. Mice were placed in the altered chamber for 5 min to measure freezing level in the altered context; and after this 5-min period, a tone (85 dB, 2 kHz) was delivered for 1 min to measure freezing to tone. Mice behavior was recorded with the FreezeFrame software and analyzed with FreezeView software (Coulbourn Instruments). Motionless bouts lasting 1 s were considered as freezing. The percentage of time animal froze was calculated, and the group means with SEM and accumulative distribution of percentage freeze were analyzed.

### Novel object location

Novel object location tests were performed, as previously described (43). Before training, mice habituated to the experimental apparatus for 5 min in the absence of objects. During habituation, animals were allowed to explore an empty arena. Twenty-four hours after habituation, animals were exposed to the familiar arena, with two identical objects added and allowed to explore for 10 min. During the retention test, mice were allowed to explore the experimental apparatus for 6 min. Exploration was scored when a mouse's head was oriented toward the object within a distance of 1 cm or when the nose was touching the object. The relative exploration time was recorded and expressed as a discrimination index [DI = $(t_{novel} - t_{familiar})/(t_{novel} + t_{familiar}) \times 100\%$]. Mean exploration times were then calculated, and the discrimination indexes between treatment groups were compared. Mice that explored both objects for 3 s in total during either training or testing were removed from further analysis. Mice that demonstrated an object preference during training (DI >±20) were also removed.

## REFERENCES AND NOTES

1. M. I. Hiskens, M. Angoa-Pérez, A. G. Schneiders, R. K. Vella, A. S. Fenning, Modeling sports-related mild traumatic brain injury in animals-A systematic review. *J. Neurosci. Res.* **97**, 1194–1222 (2019).
2. D. G. Siedler, M. I. Chuah, M. Kirkcaldie, J. C. Vickers, A. E. King, Diffuse axonal injury in brain trauma: Insights from alterations in neurofilaments. *Front. Cell. Neurosci.* **8**, 429 (2014).
3. R. Gupta, N. Sen, Traumatic brain injury: A risk factor for neurodegenerative diseases. *Rev. Neurosci.* **27**, 93–100 (2016).
4. M. A. Abd-Elfattah Foda, A. Marmarou, A new model of diffuse brain injury in rats. Part II: Morphological characterization. *J. Neurosurg.* **80**, 301–313 (1994).
5. A. Fesharaki-Zadeh, Chronic Traumatic Encephalopathy: A brief overview. *Front. Neurol.* **10**, 713 (2019).
6. P. S. Vosler, D. Sun, S. Wang, Y. Gao, D. B. Kintner, A. P. Signore, G. Cao, J. Chen, Calcium dysregulation induces apoptosis-inducing factor release: Cross-talk between PARP-1- and calpain-signaling pathways. *Exp. Neurol.* **218**, 213–220 (2009).
7. A. Yildiz-Unal, S. Korulu, A. Karabay, Neuroprotective strategies against calpain-mediated neurodegeneration. *Neuropsychiatr Dis. Treat.* **11**, 297 (2015).
8. A. Koumura, Y. Nonaka, K. Hyakkoku, T. Oka, M. Shimazawa, I. Hozumi, T. Inuzuka, H. Hara, A novel calpain inhibitor,((1S)-1 ((((1S)-1-benzyl-3-cyclopropylamino-2, 3-di-oxopropyl) amino) carbonyl)-3-methylbutyl) carbamic acid 5-methoxy-3-oxapentyl ester, protects neuronal cells from cerebral ischemia-induced damage in mice. *Neuroscience* **157**, 309–318 (2008).
9. J. Anagli, Y. Han, L. Stewart, D. Yang, A. Movsisyan, K. Abounit, D. Seyfried, A novel calpastatin-based inhibitor improves postischemic neurological recovery. *Biochem. Biophys. Res. Commun.* **385**, 94–99 (2009).
10. S. Liu, F. Yin, J. Zhang, Y. Qian, The role of calpains in traumatic brain injury. *Brain Inj.* **28**, 133–137 (2014).
11. F. H. Kobeissy, M. C. Liu, Z. Yang, Z. Zhang, W. Zheng, O. Glushakova, S. Mondello, J. Anagli, R. L. Hayes, K. K. Wang, Degradation of βII-spectrin protein by calpain-2 and caspase-3 under neurotoxic and traumatic brain injury conditions. *Mol. Neurobiol.* **52**, 696–709 (2015).
12. E. B. Cagmat, J. D. Guingab-Cagmat, A. V. Vakulenko, R. L. Hayes, J. Anagli, Potential Use of Calpain Inhibitors as Brain Injury Therapy. in *Brain Neurotrauma: Molecular, Neuropsychological and Rehabilitation Aspects*, F. H. Kobeissy, Ed. (CRC Press/Taylor & Francis, 2015), Chapter 40.
13. M. Siklos, M. BenAissa, G. R. J. Thatcher, Cysteine proteases as therapeutic targets: Does selectivity matter? A systematic review of calpain and cathepsin inhibitors. *Acta Pharm. Sin. B* **5**, 506–519 (2015).
14. Y. Ono, T. C. Saido, H. Sorimachi, Calpain research for drug discovery: Challenges and potential. *Nat. Rev. Drug Discov.* **15**, 854–876 (2016).
15. S. N. Thompson, K. M. Carrico, A. G. Mustafa, M. Bains, E. D. Hall, A pharmacological analysis of the neuroprotective efficacy of the brain- and cell-permeable calpain inhibitor MDL-28170 in the mouse controlled cortical impact traumatic brain injury model. *J. Neurotrauma* **27**, 2233–2243 (2010).
16. X.-X. Yan, A. Jeromin, Spectrin breakdown products (SBDPs) as potential biomarkers for neurodegenerative diseases. *Curr. Transl. Geriatr. Exp. Gerontol. Rep.* **1**, 85–93 (2012).
17. K. M. Schoch, C. R. Reyn, J. Bian, G. C. Telling, D. F. Meaney, K. E. Saatman, Brain injury-induced proteolysis is reduced in a novel calpastatin-overexpressing transgenic mouse. *J. Neurochem.* **125**, 909–920 (2013).
18. M. Bains, J. E. Cebak, L. K. Gilmer, C. C. Barnes, S. N. Thompson, J. W. Geddes, E. D. Hall, Pharmacological analysis of the cortical neuronal cytoskeletal protective efficacy of the calpain inhibitor SNJ-1945 in a mouse traumatic brain injury model. *J. Neurochem.* **125**, 125–132 (2013).
19. C. S. Hill, M. P. Coleman, D. K. Menon, Traumatic axonal injury: Mechanisms and translational opportunities. *Trends Neurosci.* **39**, 311–324 (2016).
20. R. Siman, N. Giovannone, G. Hanten, E. A. Wilde, S. R. McCauley, J. V. Hunter, X. Li, H. S. Levin, D. H. Smith, Evidence that the blood biomarker SNTF predicts brain imaging changes and persistent cognitive dysfunction in mild TBI patients. *Front. Neurol.* **4**, 190 (2013).
21. R. Siman, P. Shahim, Y. Tegner, K. Blennow, H. Zetterberg, D. H. Smith, Serum SNTF increases in concussed professional ice hockey players and relates to the severity of postconcussion symptoms. *J. Neurotrauma* **32**, 1294–1300 (2015).
22. Y. Wang, Y. Liu, D. Lopez, M. Lee, S. Dayal, A. Hurtado, X. Bi, M. Baudry, Protection against TBI-induced neuronal death with post-treatment with a selective calpain-2 inhibitor in mice. *J. Neurotrauma* **35**, 105–117 (2018).

23. Y. Wang, V. Briz, A. Chishti, X. Bi, M. Baudry, Distinct roles for μ-calpain and M-calpain in synaptic NMDAR-mediated neuroprotection and extrasynaptic NMDAR-mediated neurodegeneration. *J. Neurosci.* **33**, 18880–18892 (2013).

24. E. J. Perez, S. A. Tapanes, Z. B. Loris, D. T. Balu, T. J. Sick, J. T. Coyle, D. J. Liebl, Enhanced astrocytic D-serine underlies synaptic damage after traumatic brain injury. *J. Clin. Invest.* **127**, 3114–3125 (2017).

25. A. L. Petraglia, B. A. Plog, S. Dayawansa, M. Chen, M. L. Dashnaw, K. Czerniecka, C. T. Walker, T. Viterise, O. Hyrien, J. J. Iliff, R. Deane, M. Nedergaard, J. H. Huang, The spectrum of neurobehavioral sequelae after repetitive mild traumatic brain injury: A novel mouse model of chronic traumatic encephalopathy. *J. Neurotrauma* **31**, 1211–1224 (2014).

26. A. L. Petraglia, B. A. Plog, S. Dayawansa, M. L. Dashnaw, K. Czerniecka, C. T. Walker, M. Chen, O. Hyrien, J. J. Iliff, R. Deane, J. H. Huang, M. Nedergaard, The pathophysiology underlying repetitive mild traumatic brain injury in a novel mouse model of chronic traumatic encephalopathy. *Surg. Neurol. Int.* **5**, 184 (2014).

27. N. M. Kanaan, G. A. Morfini, N. E. LaPointe, G. F. Pigino, K. R. Patterson, Y. Song, A. Andreadis, Y. Fu, S. T. Brady, L. I. Binder, Pathogenic forms of tau inhibit kinesin-dependent axonal transport through a mechanism involving activation of axonal phosphotransferases. *J. Neurosci.* **31**, 9858–9868 (2011).

28. N. M. Kanaan, K. Cox, V. E. Alvarez, T. D. Stein, S. Poncil, A. C. McKee, Characterization of early pathological tau conformations and phosphorylation in chronic traumatic encephalopathy. *J. Neuropathol. Exp. Neurol.* **75**, 19–34 (2016).

29. X. Ge, J. Yu, S. Huang, Z. Yin, Z. Han, F. Chen, Z. Wang, J. Zhang, P. Lei, A novel repetitive mild traumatic brain injury mouse model for chronic traumatic encephalopathy research. *J. Neurosci. Methods* **308**, 162–172 (2018).

30. A. S. Chen-Plotkin, V. M.-Y. Lee, J. Q. Trojanowski, TAR DNA-binding protein 43 in neurodegenerative disease. *Nat. Rev. Neurol.* **6**, 211–220 (2010).

31. T. Yamashita, T. Hideyama, K. Hachiga, S. Teramoto, J. Takano, N. Iwata, T. C. Saido, S. Kwak, A role for calpain-dependent cleavage of TDP-43 in amyotrophic lateral sclerosis pathology. *Nat. Commun.* **3**, 1307 (2012).

32. Y. Wang, G. Zhu, V. Briz, Y.-T. Hsu, X. Bi, M. Baudry, A molecular brake controls the magnitude of long-term potentiation. *Nat. Commun.* **5**, 3051 (2014).

33. U. Wilhelmsson, E. A. Bushong, D. L. Price, B. L. Smarr, V. Phung, M. Terada, M. H. Ellisman, M. Pekny, Redefining the concept of reactive astrocytes as cells that remain within their unique domains upon reaction to injury. *Proc. Natl. Acad. Sci. U.S.A.* **103**, 17513–17518 (2006).

34. B. M. Davis, M. Salinas-Navarro, M. F. Cordeiro, L. Moons, L. De Groef, Characterizing microglia activation: A spatial statistics approach to maximize information extraction. *Sci. Rep.* **7**, 1576–1512 (2017).

35. B. C. Mouzon, C. Bachmeier, A. Ferro, J. O. Ojo, G. Crynen, C. M. Acker, P. Davies, M. Mullan, W. Stewart, F. Crawford, Chronic neuropathological and neurobehavioral changes in a repetitive mild traumatic brain injury model. *Ann. Neurol.* **75**, 241–254 (2014).

36. J. E. Gerson, U. Sengupta, R. Kayed, Tau oligomers as pathogenic seeds: Preparation and propagation in vitro and in vivo. *Methods Mol. Biol.* **1523**, 141–157 (2017).

37. K. Li, J. Li, J. Zheng, S. Qin, Reactive astrocytes in neurodegenerative diseases. *Aging Dis.* **10**, 664–675 (2019).

38. Y. Wang, R. A. Hall, M. Lee, A. Kamgar-Parsi, X. Bi, M. Baudry, The tyrosine phosphatase PTPN13/FAP-1 links calpain-2, TBI and tau tyrosine phosphorylation. *Sci. Rep.* **7**, 11771 (2017).

39. M. Puskarjov, F. Ahmad, K. Kaila, P. Blaesse, Activity-dependent cleavage of the K-Cl cotransporter KCC2 mediated by calcium-activated protease calpain. *J. Neurosci.* **32**, 11356–11364 (2012).

40. N. Gorgoraptis, L. M. Li, A. Whittington, K. A. Zimmerman, L. M. Maclean, C. McLeod, E. Ross, A. Heslegrave, H. Zetterberg, J. Passchier, P. M. Matthews, R. N. Gunn, T. M. McMillan, D. J. Sharp, In vivo detection of cerebral tau pathology in long-term survivors of traumatic brain injury. *Sci. Transl. Med.* **11**, eaaw1993 (2019).

41. A. A. Walf, C. A. Frye, The use of the elevated plus maze as an assay of anxiety-related behavior in rodents. *Nat. Protoc.* **2**, 322–328 (2007).

42. A. Can, D. T. Dao, C. E. Terrillion, S. C. Piantadosi, S. Bhat, T. D. Gould, The tail suspension test. *J. Vis. Exp.* **2012**, e3769 (2012).

43. Y. Liu, J. Sun, Y. Wang, D. Lopez, J. Tran, X. Bi, M. Baudry, Deleting both PHLPP1 and CANP1 rescues impairments in long-term potentiation and learning in both single gene knock-out mice. *Learn. Mem.* **23**, 399–404 (2016).